

Investigation of the UAV Capability for Measuring Building's Cracks Dimensions

Farsat Heeto Abdulrahman ^{1,a} and Sarhat M. Adam^{1,b}

¹Department of Surveying Engineering, College of Engineering, University of Duhok.

ABSTRACT

This research uses Unmanned Aerial vehicles (UAVs) as a platform to examine and monitor a building. It concentrates on inspecting building flaws, particularly cracks, utilizing UAV photogrammetry, which is the focus of this study. The reason for using a building as an object in this work is that the building maintenance team can evaluate, which can support providing trustworthy crack information on buildings. The building chosen for this work contains a reasonable amount of cracks, making it suitable. The methodology and procedures are used to take images of cracks in the building. The software can determine the size of the cracks based on 518 photos taken with a UAV. The 3D model of the building is created by using Agisoft Photoscan software to receive an overview of the building dimensions. The measurement of cracks is also being processed using Photomodeler software. The results showed that the capability of the UAV imagery can aid present surveying operations, particularly on building maintenance. It also indicates that cracks appeared on buildings from 0.72cm to 3.24cm in a certain altitude. The Root Mean Square (RMS) error obtained from comparing the actual and measured value of cracks was ± 0.70 cm with the help of 114 GCPs distributed all over the building.

KEYWORDS: Building; Crack; Measurement; Assessment; Accuracy; 3D; image; photogrammetry; UAV

1 INTRODUCTION

The detection of cracks is defined as a process in which cracks are detected in a building, especially walls, roofs, and other concrete surfaces. There are two ways in which this process can be carried out, which are destructive and nondestructive. The manual crack detection mechanisms demonstrate difficulty for various reasons such as expert availability, time consumption, etc. Thus, an automated mechanism for crack detection from buildings has been adopted. The performance of this system is much more improved than manual systems in terms of speed, efficiency, and accuracy.

The use of image processing techniques improves the accuracy of the automated system. Researchers have offered a variety of image processing approaches, which could replace visual methods because they are not created in an on-site setting. However, there are multiple difficulties when detecting cracks by image processing due to image quality, image size, pixel combination of photos, image noise, blurred images, and irregular images captured by the camera. Also, the effect of lighting on images can pose issues in image processing techniques. This factor has an impact on technique accuracy since it degrades image quality. This research focuses on investigating the cracks in a building by using UAV as a tool with photogrammetry as a recommended technique.

2 RELATED WORK

The state of buildings is monitored by conventional means, by man-driven visual assessment only, which may incorporate some tape testing. Eschmann (2012) mentioned that information on cracking conditions and separation of the covering layers of concrete or stone-based structures can be provided through traditional monitoring. Choi et al. (2021) detected damages such as moisture or biological changes on monument surfaces in the documentation and analysis of historical buildings. Fan et al. (2018) characterized and defined building defects by investigating the building pathology. The authors also mentioned that the conventional methods were subjected to procedures and interpretation. Photogrammetry mapping was also utilized in their study to quantify the flaws in building façades such as mortar spalling and cracks. Photogrammetry mapping was accomplished using three different techniques which were manual, semi-automatic, and automatic. Standard practices characterized the building defects. The authors were able to characterize the building defects for maintenance purposes successfully.

Bhowmick et al. (2020) stated that throughout the inspection of buildings, the 3D terrestrial laser scanning (TLS) approach was used. Using a high-resolution digital surface model (DSM) to define the levels of detail, one and two. These levels of detail were related to the polygons of the building and ceiling shapes (Qiao et al., 2021). Their study uses images from a worldview satellite with 36 cm resolution to complete the model for the 3D view. The combination of aerial imagery and LiDAR, Light Detection and Ranging is extremely beneficial in reconstructing a 3D building model. Accurate geometry and fine details resulted from the 3D building model produced in their study. Furthermore, dataset integrations were automatically used to solve the missing borders and rooftop patches.

A vast majority of damages can affect the materials of a building. Therefore, the main task in documenting work is distinguishing between these damages and their development at the period. Wei et al. (2019) stated that manual damage mapping is costly and time-consuming. Furthermore, the gathered information is affected by the accessibility of the structure, its location and dimensions, as well as the method of assessment and examination (Reisner-Kollmann, 2013). According to Meena et al. (2013), the analysis defines a methodology for evaluating various flaws using independent criteria such as area, position, and dimension. It also considers the direction of the building's facade, such as cracks in mortar, paint flaking, paint, and mortar spalling. It uses photogrammetry photos to avoid inspection errors caused by user knowledge or estimation.

Recently, the study conducted by (Ab Rahman and Tahar, 2022) mentioned that the inspection of buildings' cracks using UAV imagery at a certain altitude could be powerful for crack detection within the 80-centimeter level of accuracy. Also, (Alidoost et al., 2015, and Remondino et al., 2012) verified that photogrammetric measurements in various application fields of UAVs have demonstrated great potential over classical manned aerial photogrammetry. It has GPS/INS sensors and can fly in manual, semi-automatic, and automated modes (Colomina et al., 2014). The integrated GPS/INS provides the parameters to facilitate and refine the correct camera posture and attitudes required. Qu et al. (2019) mentioned that uncrewed aircraft hovering and landing do not require a wide area or ground. Thus, Hundreds of square meters of playgrounds, grass meadows, or even a hundred-meter part of straight streets are adequate.

Collecting real-time close-range imagery, cost-efficiency, and promising accuracy are the main advantageous features of the UAV system, making it much cheaper than laser scanners and most precise surveying techniques. In addition, the hiring cost is also saved compared to other surveying methods, as the UAV system needs minimum specialists for data collection (Lucieer et al., 2014). Furthermore, as long as the UAV mapping follows the correct procedures, it could yield accuracy up to the centimetre level (Siebert and Teizer, 2014). It is impossible to obtain a complete stereo coverage of the entire building by using terrestrial images due to building heights.

The existing technique utilized for observing the status of buildings is through man-driven visual examinations, which are normally appraised by visual inspections. According to Murtiyoso et al. (2014), expensive cost or scaffolding is no longer required to inspect building defects. Rodríguez et al. (2015) summarized the current crack measurement approaches such as visual inspection, image processing, intelligent film methodology, and circulated optical fibre. The approaches mentioned are being used for the width, location, and initiation of cracks. Otherwise, traditional crack monitoring is costly and time-consuming. This research is motivated to improve the method of image-obtaining for image processing techniques. Most inaccessible constructions can be provided with a series of high-resolution photos or high-definition video by UAV. It may also observe the images on the screens of the remote ground stations to ensure that the correct photographs are acquired. Work labour involves significantly less effort, making the proposition more appealing (Nex and Remondino, 2014). Close-range photogrammetry can assist users in identifying and measuring cracks in buildings. High-rise buildings are challenging to approach manually, and it is also impossible to detect crack features. Therefore, UAVs may analyze and assess specific cracks quickly and uncomplicatedly. The purpose of this research is to explore building cracks using UAV imagery.

Kattan et al. (2022) studied geometric and visual inspections on a large building. The accurateness of the geometric of the selected points on the building, the maximum standard deviation in the coordinates was $\pm 4\text{cm}$. The relative accuracy in distance measurements ranged from 0.72% to 4.92%. Also, the accuracy of the outcome of UAV images was addressed compared to the aerial survey system by (ABDULRAHMAN et al., 2020). The purpose is to calculate the estimated accuracy of the orthophoto created from the outcome of UAV images encountered to the present orthophoto created from an aerial survey implemented by Vossing German Company in Duhok city, 2011, using GPS ground control point as a reference base of the same tested area of Duhok university Campus, Duhok, Kurdistan region, Iraq. This study investigates the capability of UAVs in crack detection and the geometric accuracy of the detected crack in measuring length and width compared to the manual method.

3 METHODOLOGY AND PLANNING

This study methodology is composed of four parts as follows:

Part one: a primary work and literature review

Part two: Data collection with three fundamental subjects: crack detection, camera self-calibration, and flight planning. Part two is one of the essential parts, and the majority of time is spent on this part to acquire good-quality data.

Part three: Data processing using suitable software

Part four: Data analysis involving crack detection, the 3D model, and crack evaluation.

Concerning the Planning of this work, two methods were used to accomplish the aim, which were 3D modelling of the building and measuring the crack. The former method is producing the 3D model of the building for the outline dimension. The latter method is through crack detection, where the measurement of the crack is specified. These approaches were done through the following steps.

- Measuring the GCPs around the building using the GPS-RTK method from a known point (C12).
- Measuring the GCPs on the building by placing targets on walls and windows of the building to measure the target's coordinates using the Total Station (TS02) instrument.
- Flying the UAV around all the sides and the top of the building. Also, it is used to capture images of the crack in the building.
- Agisoft Photoscan is used for modeling the building. The cracks were manually detected and measured via visual inspection using Photomodeler software.
- Assessing the crack measurements gained from the UAV images using the photogrammetric techniques.

4 STUDY AREA AND DATA COLLECTION

The work was carried out at the University of Duhok Campus, College of Engineering, and used as a case study for crack detection. The location, as shown in Figure 1, is the outline of the building that requires checking for cracks. The research involves creating a 3-D model of a three-story building using a photogrammetric method. The structure is 6965 square meters. It stands 13.75m tall. The building's overall length is 85m, with widths ranging from 19.70m on one side to 43.3m on the other. The entrance and lobby of the building are circular in design, with a diameter of 23.40m. This section's upper ceiling features a light translucent dome 7.5m in diameter and 2.6m in height. Most of the upper roof surface is taken up by air-conditioning system pipes, units, and water storage tanks. The structure features 330 windows spread across three sides. Tall trees concealed parts of the building's Northern and Eastern sides, obscuring imaging and control observations.



Figure 1: University of Duhok Campus, College of Engineering

a. Control Points

Nine ground control points were constructed around the building. 60*60 cm flex-painted targets were used to designate the points. The coordinates of these points were determined using GPS measurements made with a Leica Viva GNSS, a GS10 base receiver, and a GS15 rover receiver. The system's accuracy at a single base is given as $\pm 8\text{mm} \pm 1 \text{ ppm}$ for the horizontal component and $\pm 15\text{mm} \pm 1 \text{ ppm}$ for the vertical component. The GS10 GNSS receiver was installed on a known control (C12) point in the study region. As illustrated in Figure 2, the GNSS GS15 receiver was employed as a rover station for measuring and recording data on the 9 GCPs dispersed around the building.



Figure 2: Study area overlain measured GCP's

The WGS84, UTM-38N projection was utilized as the coordinate system for measurements. Figure 3a shows 99 targets, self-adhesive 10*10 cm, installed as control points on the external walls and windows of the building. The targets were set evenly to cover all control points throughout the building. The Leica TS02 total station in the reflector-less mode determined these points' coordinates. The TS02 has an accuracy of $\pm 3''$ in measuring angle, an accuracy of distance of $\pm 2\text{mm} \pm 2\text{ppm}$, and a range measurement of 80m in the reflector-less mode, according to the manufacturer specs.

Figure 3b shows the total station positioned on the 5 GCPs measured by GPS in RTK mode, from which self-adhesive targets were observed and recorded using the SD card memory attached to the device. Each GCP was named according to each side of the building. For example, all the GCPs (S1, S2, S3, etc.) are for the side of the garage in the South direction. Other sides of the building in the North, East, and West direction are named (N, E, and W) respectively. Also, 19 points were selected on the roof, and the GS15 rover receiver measured their coordinates. A total of 128 GCP coordinates for the selected building were measured to generate a 3D model of the building.

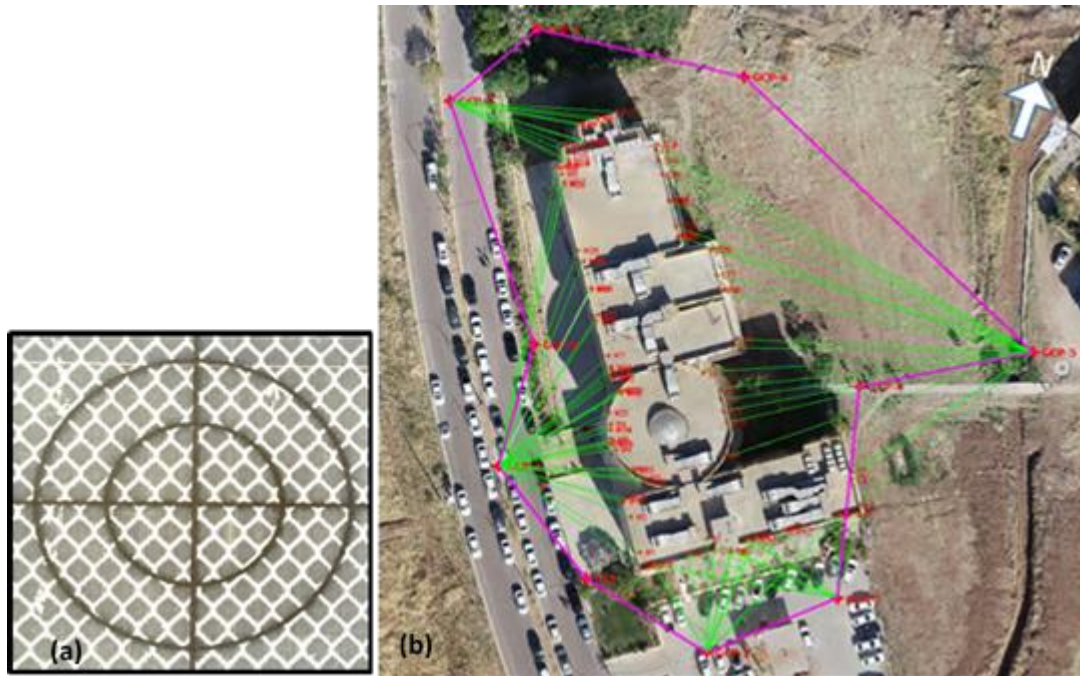


Figure 3: a.) target, self-adhesive. B.) The position of TS02 and distribution of GCPs

b. UAV camera specification

The UAV Phantom 4 Pro, 4K- DJI was used as a platform for the imaging camera. Table 1 shows the camera and imaging settings.

Table 1. The setting of flight and camera parameters

Camera Model	FC6310 (8.8mm)
Focal Length	8.8 mm
Pixel Size	2.41 x 2.41 μm
Ground sample distance (GSD)	1.97 cm/pixel
Side Overlap Ratio (%)	70%
Frontal Overlap Ratio (%)	75%
Side Overlap Ratio (Oblique)	70%
Resolution (pix)	5472 W x 3648 H

c. Flight planning, imaging, and processing

A total of 518 photos were taken of the structure and its surroundings. DJI Capture in the software was utilized for flight planning. The coverage was obtained during two flights. One flight was oblique, while the other was vertical. The vertical flight has five strips above the building, as indicated in Figure 4 a. The oblique flight was programmed to take photographs 86.31m distant from the front of the building façades at an altitude of 24.90m above ground level, with a camera depression angle of 60° from the horizon, as illustrated in Figure 4, b.

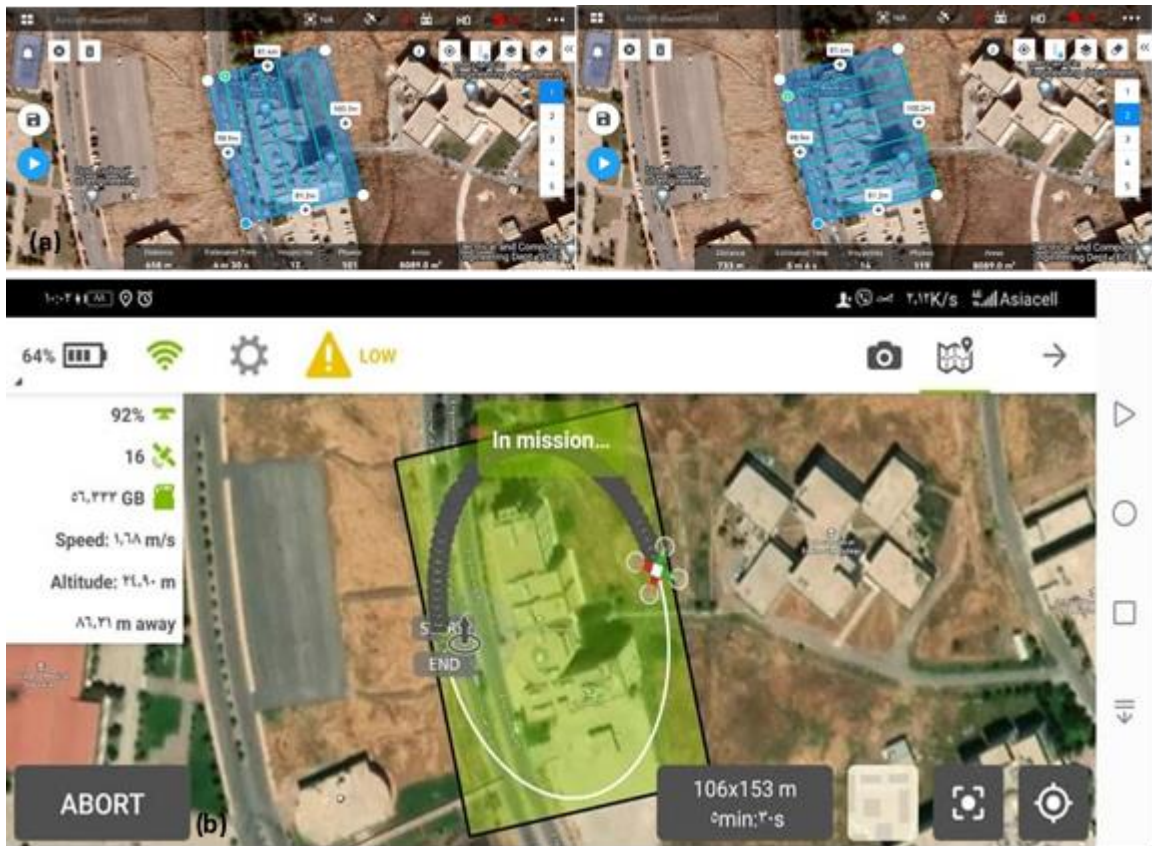


Figure 4: Flying Strips. a.) vertical images, five strips above the building. b.) oblique images

The Agisoft Photo Scan software was used to process the data and create the 3-D model of the building. The 518 photos and 128 markers, ground control points were used as input. Figure 5 depicts the processing flow diagram. After aligning the images, selecting control points on the overlapped images is one stage in generating a 3-D model in Agisoft Photoscan. When a location on the first image is selected,

the epipolar line appears, passing through the matching point on the second image. This procedure will reflect the level of matching precision. Table 2 shows the generated data details.

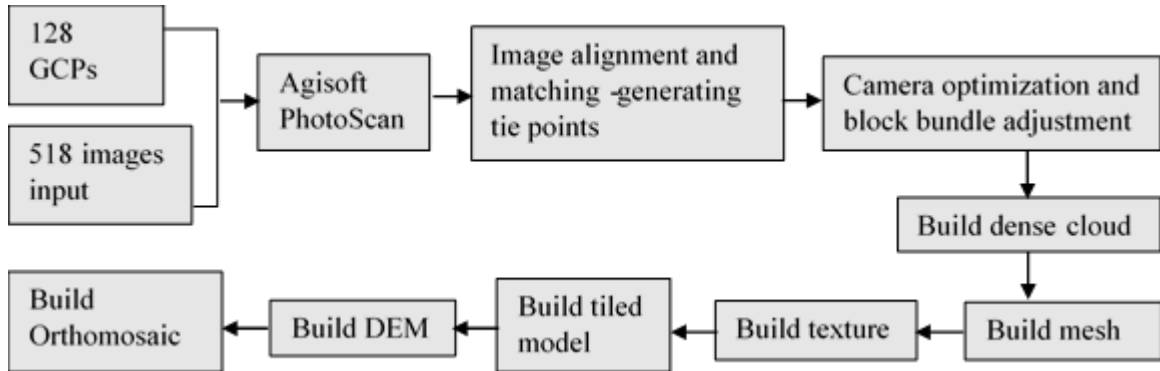


Figure 5: The workflow diagram of Agisoft Photoscan software

Table 2. Indicates the details of the created data.

Tie points	269,165 points
Dense cloud	7,825,850 points with medium quality
3D model	1,545,170 faces and 774,335 vertices
Tiled model	1.15 cm/pix
DEM	5,076 x 5,800 at a 4.59cm/pix
Orthomosaic	20,304 x23,196 pixels at a 1.15cm/pix

Figure 6 depicts the active window of Agisoft PhotoScan. The window can display the chosen image, the 3D model, the workflow, the image perspective centers, and the details of the GCPs.

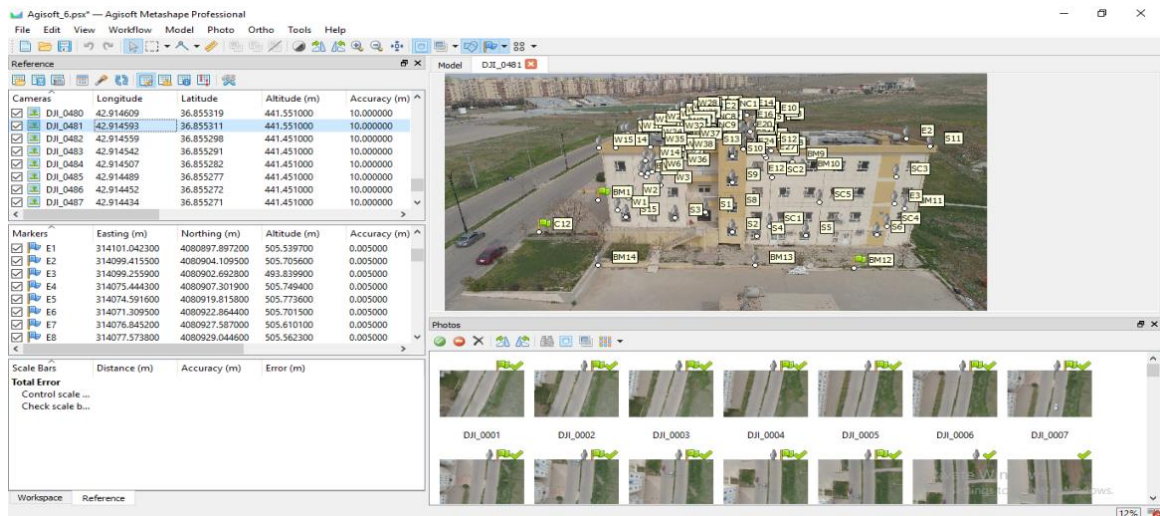


Figure 6: Active window of Agisoft PhotoScan software

Table 3 displays the report of the RMS error of the 128 GCPs after various refinement phases by adding control points, block bundle adjustment, and camera calibration parameters. The total RMSE does not reach $\pm 5\text{cm}$, which is a reasonable value given the project's size and scope.

Table 3. After-refinement, RMSE of the measured GCPs

Pts.No.	X	Y	Z	XY	Total	Image
128	$\pm 3.440\text{ cm}$	$\pm 2.600\text{ cm}$	$\pm 1.890\text{ cm}$	$\pm 4.310\text{ cm}$	$\pm 4.710\text{ cm}$	$\pm 0.490\text{ cm}$

The dense cloud medium-quality process takes around 2 hours. The tiled model is shown in Figure 7a, and the tiled model with a GCPs marker is shown in Figure 7b



Figure 7: a.) The tiled model. b.) The tiled model overlains control points

The AgisoftPhotoScan permits the building of a digital elevation model (DEM) with a density of point 5,076 x 5,800 and a resolution of 4.59 cm/pix. Different elevation ranges are assigned different colours, as shown in Figure 8, a. The Ortho-mosaic created with 28795x28835 pixels at a resolution of 1.19 cm/pix is shown in Figure 8b.

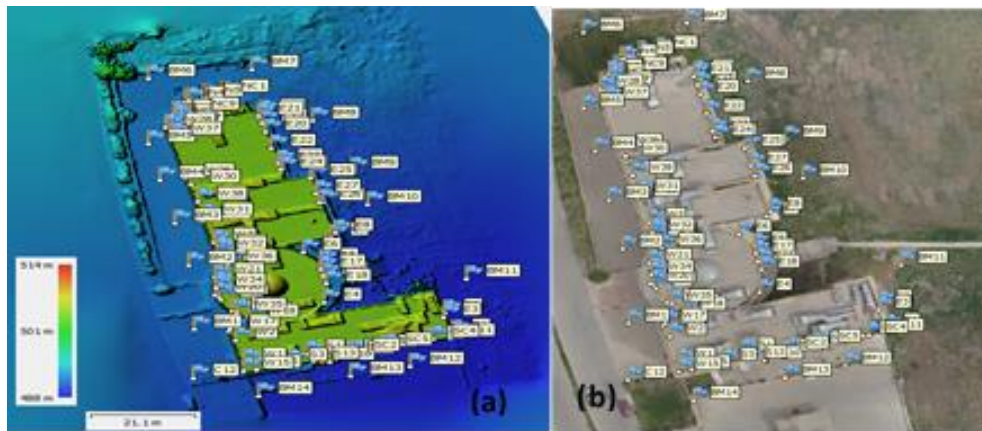


Figure 8: a.) Colour-coded of the DEM overlain control point. b.) The ortho-mosaic overlain control points

As previously stated, only clean and sharp photos were chosen from the processing data and utilized to generate the 3D model as an outline of the building using Agisoft Photoscan software. As a result, a 3D

model can show an outline of the building dimensions in different directions. As illustrated in Figure 9, the outline dimension of the building was built to indicate the location of the crack on the building.

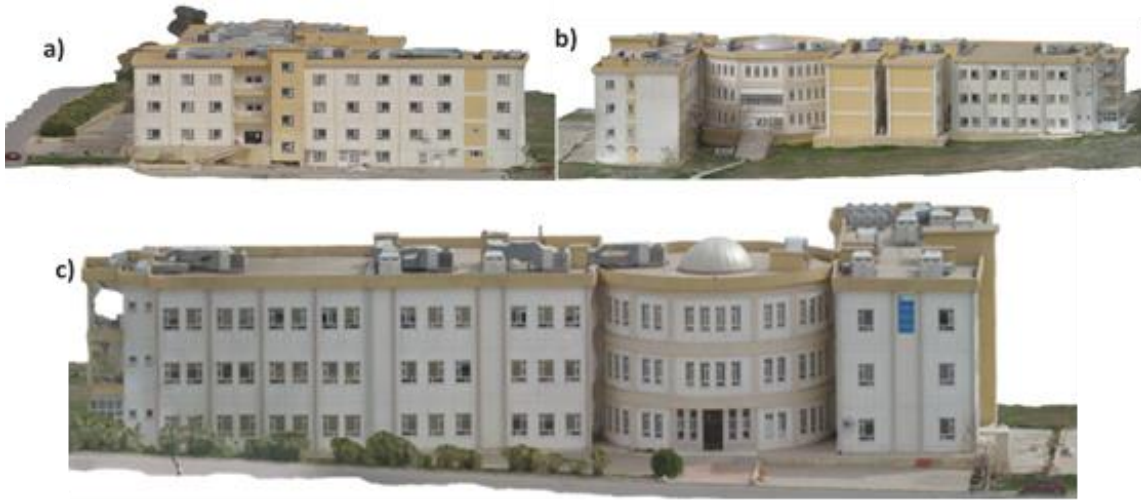


Figure 9: Direction of building a) south view, b) East view, c) West View

These directions of the 3D model are then exported to a Photomodelor software to measure crack width and length in each direction side of the building. Figure 10 shows a sample of different types of cracks on the building for each side (South, North, East, and West) using 3D model.

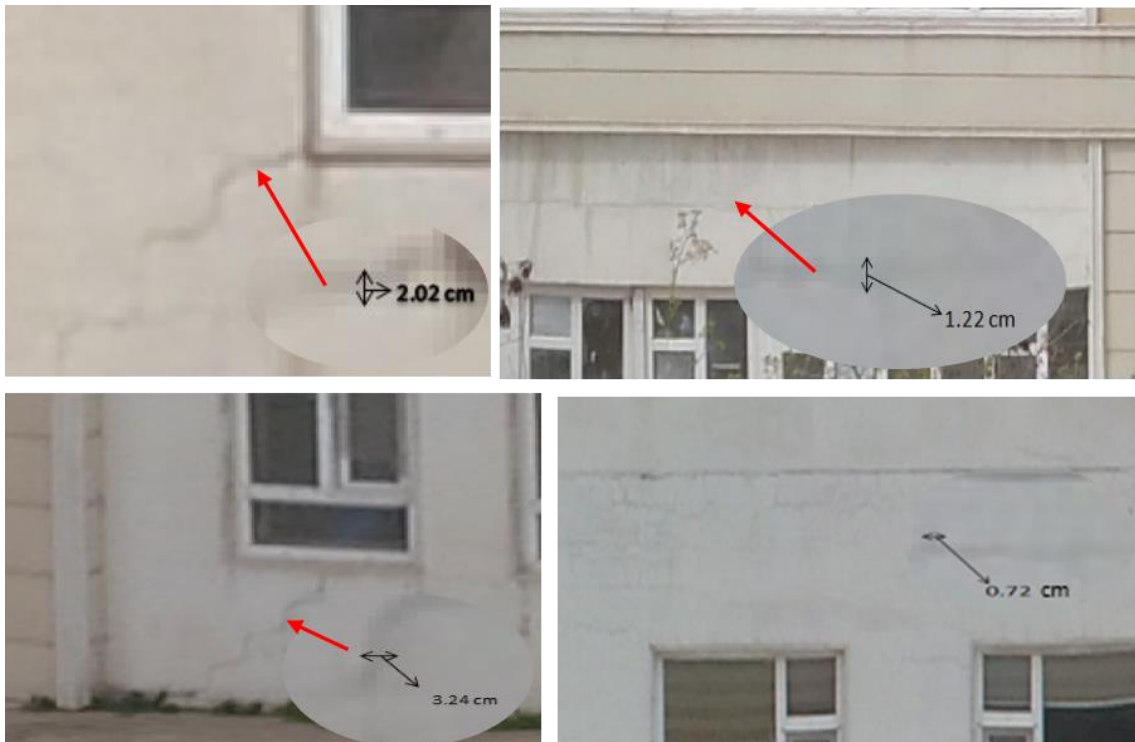


Figure 10: Sample of Measuring crack width and length in the Photimodelor software

5 ACCURACY CHECK

The 3D model created by the Photomodelor software is used to check the geometrical accuracy. It was possible to put the pointer anywhere on the model, measure the crack width and length, as shown in Figure 10, and compare these widths with the conventional measuring crack using tape. The width of a crack in all directions of the building facades was measured; the focus was on those accessible cracks for measuring by tape. The difference in errors between the two sets of measuring is illustrated in Table (5). The standard deviation on any of the four sides of the building crack is less than ± 0.7 cm.

Table 5. Crack's Measurement on the South and East Side of Building

Position of crack-south	True width (cm)	Measured width (cm)	Discrepancy (cm)-South	Position of crack- East	True width (cm)	Measured width (cm)	Discrepancy (cm)-East
S1	1.4	1.61	0.3	E1	1.1	1.61	-0.51
S2	1.9	1.18	0.29	E2	1.6	2.94	-1.34
S3	2	1.72	0.82	E3	1.2	2.10	-0.9
S4	2	2.02	0.28	E4	1.7	1.22	0.48
S5	2.5	2.04	0.48	E5	2	1.83	0.17
S6	1.5	0.72	-0.54	E6	2	1.93	0.07
S7	1	2.10	0.28	E7	1	1.91	-0.91
S8	1.2	2.30	-0.9	E8	2	1.97	0.03
S9	1.2	2.05	-1.1	E9	2.3	1.53	0.77
S10	2.5	1.37	0.45	E10	2.5	2.02	0.48
	1.72	1.684			1.74	1.906	
	Stdv.		0.6442				0.7076

Table 6. Crack's Measurement on the West and North Side of Building

Position of crack- West	Actual width (cm)	Measured width (cm)	Discrepancy (cm)-West	Position of crack- North	Actual width (cm)	Length (cm)	Discrepancy (cm)-North
W1	2	1.65	0.35	N1	1.3	1.10	0.2
W2	2.5	1.18	1.32	N2	1.4	0.98	0.42
W3	2.2	1.80	0.4	N3	2.7	2.10	0.6
W4	1	1.91	-0.91	N4	1.6	1.42	0.18
W5	3.6	3.24	0.36	N5	3.2	3.20	0
W6	2	1.79	0.21	N6	2	2.74	-0.74
W7	2.5	1.96	0.54	N7	1.9	2.38	-0.48
W8	2	1.57	0.43	N8	1.2	1.62	-0.42
W9	1.3	1.83	-0.53	N9	2	1.85	0.15
W10	2.3	1.36	0.94	N10	1.7	0.76	0.94
		1.829				1.815	
	Stdv.		0.6412				0.5161

Tables 5 and 6 show the maximum crack width in all directions: South, East, North, and West are about 3.20, 2.30, 2.94, and 3.24, respectively. The minimum Crack width was 0.76, 0.72, 1.22, and 1.18, respectively. The mean of the measurement crack measure for all sides of the building is 1.81 cm. this statistic means that the capability of UAVs in crack detection cannot show on a wall building with less than

0.72 cm. Also, the standard deviation of the discrepancy between the actual and measured value can be shown in Figure 11.

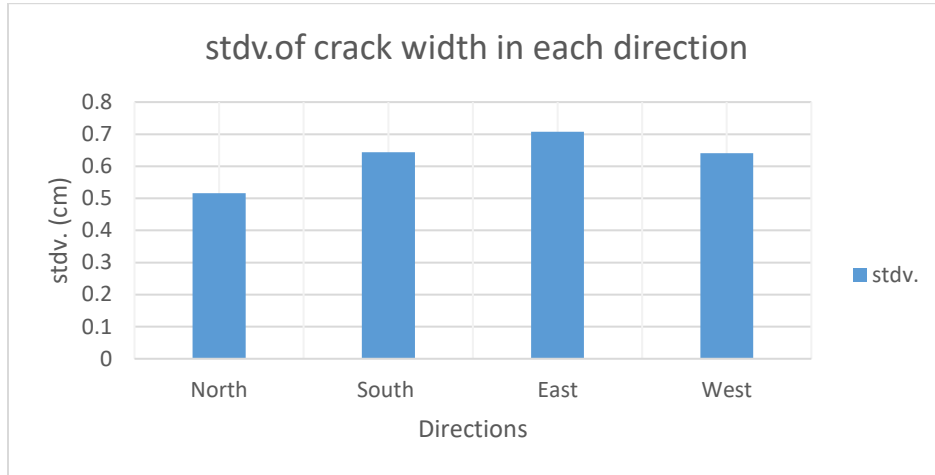


Figure 11: standard deviation of the discrepancy in building direction

Geometrical accuracy was further checked by measuring five crack lengths from each side directly on the building with tape and comparing these distances to the length measured on the 3D model built using the Photomodeler software, as shown in Table 7.

Table 7. shows the differences in five crack distances measured directly and on the model

Distance	Actual Distance (cm)	Model distance (cm)	Discrepancy (cm)	Relative discrepancy
1	32	31.8	-0.2	-0.63%
2	61	61.4	-0.4	-0.65%
3	162	161.3	-0.7	-0.43%
4	69	68.5	-0.5	-0.73%
5	151	153	2	1.31%

According to Table 7, the differences between the tape measured and model distances range between -0.2 and 2 cm, with a relative error ranging from -0.43% to 1.32%.

6 DISCUSSION

- Crack identification for large-scale infrastructure is proposed by adopting the UAV with image processing. Image processing model for detecting crack problems on building structures' surfaces. The digital photos used for crack analysis had several issues, including low contrast, inconsistent illumination, and noise pollution.
- Buildings with regular shapes necessitate vertical (nadir) and oblique image coverage. Because of the absence of vertical coverage, model deformation is to be expected. When GCPs are added for the Geo-referencing process in AgisoftPhotoscan, the images on which points are chosen show all of the control points on the front and back sides (Kattan et al., 2022). Figure 17 depicts the building of the East façade image under processing and the position of the control points. Besides the east side control points, the west and south facade control points are visible. The study team observed

the exact comment on the building model. This issue could be regarded as a disadvantage in the software design to be tackled, as the model seems transparent, revealing all sides of the control points.



Figure 17: Revealing all sides of the control points: The East side, the West, and South facades

- Instead of using TS device, reflectorless with ground control points to measure control points on the facades, an RTK receiver can be placed on board the UAV to obtain more accurate exposure center coordinates for use in performing the intersection. UAV-RTK reduces the amount of ground control points necessary.
- A Photogrammetry method has been used for detecting the crack; the image quality and illumination are vital. These two factors significantly affect crack detection. Also, the structure complexity, like hiding corners or facades, as more difficult for using UAVs for detecting processes. Other methods may have been suggested, such as using terrestrial images.
- The building façade is divided into four sides: North, South, East, and West. When the targets measured, to make it easier for the names of marks, like if it was for South named S1, S2, etc., for North N1, N2, etc., according to how many targets exist.
- Non-metric cameras can be used to acquire images of façade occluded by trees as a first step toward overcoming model deformation caused by hidden details.
- This research summarized that cracks can be detected on the Building's façade from 0.72cm to 3.24cm using a certain UAV altitude see Table 5 and Table 6.

7 CONCLUSION

There are numerous methods for capturing photos of architectural flaws. The main emphasis of this investigation was the UAV platform used to acquire photos of cracks. The first goal was met when photos of cracks in the building were captured using a UAV. There are a few more steps to obtain higher-quality photos of faults. Flight planning is vital in ensuring that the task goes off without a hitch. Also, it prevents the UAV from collapsing or any other risk that could raise safety concerns. The outcomes demonstrated that the UAV imagery technique can be used to monitor building defects. This study also met the second goal, which was to evaluate the accuracy of defect measurement based on UAV outcomes. The crack measurement can be done correctly by utilizing the Photomodeler Scanner software. Despite a few variations between the traditional and UAV imagery methodologies, the findings were satisfactory. The

variations were slight, and the technique proved highly effective. The study also demonstrated that employing a UAV as a platform is a favorable and cost-effective strategy for obtaining real-time and close-range imagery. Because the height of buildings cannot be reached to cover the entire structure with terrestrial photos, because it is a straightforward and quick solution to accomplish the demand for full coverage, the UAV platform can be utilized for investigation or monitoring. Using the PhotoModeler software, this study achieved a crack width measurement accuracy of 0.7cm.

The Agisoft Photoscan software is extremely beneficial for 3D modeling. More photos will result in better outcomes. It makes no difference how many photos are captured as long as the entire object is covered. It is advised to gain some measurable reference scales. For instance, the window frame was employed as a reference scale in the PhotoModeler software in this work. With the overlapping photos, all measurements may be taken from that scale.

For future research, a Machine learning (ML) algorithm is required for complexity and huge structured areas. In addition, the automatic detection of the crack and calculating the size of the crack in terms of length and width is recommended for investigation in future research.

8 ACKNOWLEDGMENTS

The authors wish to thank Surveying Engineering Department, college of Engineering, University of Duhok for their support.

REFERENCES

1. AB RAHMAN, K. & TAHAR, K. N. Possibility the use of UAV platform for building's crack length measurement. IOP Conference Series: Earth and Environmental Science, 2022. IOP Publishing, 012006.
2. ABDULRAHMAN, F. H., KATTAN, R. A. & GILYANA, S. M. J. J. O. D. U. 2020. A Comparison between Unmanned Aerial Vehicle and Aerial Survey Acquired in Separate Dates for the Production of Orthophotos. 23, 52-66.
3. ALIDOOST, F., AREFI, H. J. T. I. A. O. T. P., REMOTE SENSING & SCIENCES, S. I. 2015. An image-based technique for 3D building reconstruction using multi-view UAV images. 40, 43-46.
4. BHOWMICK, S., NAGARAJAIAH, S. & VEERARAGHAVAN, A. J. S. 2020. Vision and deep learning-based algorithms to detect and quantify cracks on concrete surfaces from UAV videos. 20, 6299.
5. CHOI, D., BELL, W., KIM, D. & KIM, J. J. S. 2021. UAV-driven structural crack detection and location determination using convolutional neural networks. 21, 2650.
6. COLOMINA, I., MOLINA, P. J. I. J. O. P. & SENSING, R. 2014. Unmanned aerial systems for photogrammetry and remote sensing: A review. 92, 79-97.
7. ESCHMANN, C. 2012. Unmanned aircraft systems for remote building inspection and monitoring.
8. FAN, Z., WU, Y., LU, J. & LI, W. J. A. P. A. 2018. Automatic pavement crack detection based on structured prediction with the convolutional neural network.

9. KATTAN, R., ABDULRAHMAN, F. H., GILYANA, S. M. & ZAYA, Y. Y. J. J. O. E. R. 2022. 3D modelling and visualization of large building using photogrammetric approach. 10.
10. LUCIEER, A., JONG, S. M. D. & TURNER, D. J. P. I. P. G. 2014. Mapping landslide displacements using Structure from Motion (SfM) and image correlation of multi-temporal UAV photography. 38, 97-116.
11. MEENA, Y., MITTAL, A. J. I. J. O. A. R. I. C. S. & ENGINEERING, S. 2013. Blobs and cracks detection on plain ceramic tile surface. 3, 647-652.
12. MURTIYOSO, A., REMONDINO, F., RUPNIK, E., NEX, F., GRUSSENMEYER, P. J. T. I. A. O. T. P., REMOTE SENSING & SCIENCES, S. I. 2014. Oblique aerial photography tool for building inspection and damage assessment. 40, 309-313.
13. NEX, F. & REMONDINO, F. J. A. G. 2014. UAV for 3D mapping applications: a review. 6, 1-15.
14. QIAO, W., MA, B., LIU, Q., WU, X. & LI, G. J. S. 2021. Computer vision-based bridge damage detection using deep convolutional networks with expectation maximum attention module. 21, 824.
15. QU, Z., CHEN, Y.-X., LIU, L., XIE, Y. & ZHOU, Q. J. I. A. 2019. The algorithm of concrete surface crack detection based on the genetic programming and percolation model. 7, 57592-57603.
16. REISNER-KOLLMANN, I. 2013. *Reconstruction of 3D models from images and point clouds with shape primitives*. Technische Universität Wien.
17. REMONDINO, F., BARAZZETTI, L., NEX, F., SCAIONI, M., SARAZZI, D. J. T. I. A. O. T. P., REMOTE SENSING & SCIENCES, S. I. 2012. UAV photogrammetry for mapping and 3d modeling—current status and future perspectives. 38, 25-31.
18. RODRÍGUEZ, G., CASAS, J. R., VILLABA, S. J. S. M. & STRUCTURES 2015. Cracking assessment in concrete structures by distributed optical fiber. 24, 035005.
19. SIEBERT, S. & TEIZER, J. J. A. I. C. 2014. Mobile 3D mapping for surveying earthwork projects using an Unmanned Aerial Vehicle (UAV) system. 41, 1-14.
20. WEI, X., YANG, Z., LIU, Y., WEI, D., JIA, L. & LI, Y. J. E. A. O. A. I. 2019. Railway track fastener defect detection based on image processing and deep learning techniques: A comparative study. 80, 66-81.